AJNR

Role of 3D Pseudocontinuous Arterial Spin-Labeling Perfusion in the Diagnosis and Follow-Up in Patients with Herpes Simplex Encephalitis

R. Li, P.-A. Shi, T.-F. Liu, Y. Li, Y. Wang, K. Wu, X.-J. Chen, H.-F. Xiao, Y.-L. Wang, L. Ma and X. Lou

AJNR Am J Neuroradiol 2019, 40 (11) 1901-1907
doi: https://doi.org/10.3174/ajnr.A6279
http://www.ajnr.org/content/40/11/1901

Role of 3D Pseudocontinuous Arterial Spin-Labeling Perfusion in the Diagnosis and Follow-Up in Patients with Herpes Simplex Encephalitis

R. Li, P.-A. Shi, T.-F. Liu, Y. Li, Y. Wang, K. Wu, X.-J. Chen, H.-F. Xiao, Y.-L. Wang, L. Ma, and X. Lou

ABSTRACT

BACKGROUND AND PURPOSE: Early diagnosis and treatment of herpes simplex encephalitis are crucial to reduce morbidity and mortality. Our aim was to investigate the role of 3D pseudocontinuous arterial spin-labeling in herpes simplex encephalitis.

MATERIALS AND METHODS: From 2014 to 2019, seventeen consecutive patients with herpes simplex encephalitis and 15 healthy volunteers were recruited in the study. Conventional MR imaging and 3D pseudocontinuous arterial spin-labeling were performed in all subjects. According to the disease duration, the lesions were classified into 3 groups, including acute, subacute, and chronic stages, respectively. Clinical, neuroradiologic, and follow-up features were studied. The normalized lesion/normal tissue CBF values of lesions at different stages were measured and compared with those in the control group, respectively.

RESULTS: Compared with the control group, herpes simplex encephalitis demonstrated hyperperfusion in 11 acute cases and 6 subacute cases and hypoperfusion in 6 chronic cases. The mean normalized lesion/normal tissue CBF values of the lesions were 2.68 ± 0.54 in the acute stage, 2.42 ± 0.52 in the subacute stage, and 0.87 ± 0.30 in the chronic stage, respectively. The mean normalized lesion/normal tissue CBF values of acute and subacute lesions were significantly higher than those of the control group (1.33 ± 0.08; $P < .001$, respectively), while the mean normalized lesion/normal tissue CBF values of chronic lesions were lower than those of the control group ($P < .05$). Gradual perfusion reduction on serial 3D pseudocontinuous arterial spin-labeling was observed in herpes simplex encephalitis after effective therapy.

CONCLUSIONS: Conventional MR imaging remains most helpful in the diagnosis of herpes simplex encephalitis, while 3D pseudocontinuous arterial spin-labeling could be an adjunctive technique by providing dynamic CBF features at different stages in herpes simplex encephalitis.

ABBREVIATIONS: ASL = arterial spin-labeling; 3D-pCASL = 3D pseudocontinuous ASL; HSE = herpes simplex encephalitis; HSV = herpes simplex virus; MELAS = mitochondrial encephalopathy with lactic acidosis and stroke-like episodes; nCBF = normalized lesion/normal tissue CBF

Viral encephalitis is a life-threatening infectious disease that can occur at any age.[1] More than 100 different viruses can result in acute encephalitis;[2] however, herpes simplex encephalitis (HSE) caused by the herpes simplex virus (HSV) is the most frequent and serious sporadic form of acute viral encephalitis all over the world, accounting for about 20% of all viral encephalitis cases.[3] Of all HSE cases, nearly 90% are caused by herpes simplex virus type 1 (HSV-1) and 10% by herpes simplex virus type 2 (HSV-2).[4] The death rate has dropped dramatically since antiviral drugs have been widely used; however, some patients survive with severe neurologic sequelae like epilepsy, cognitive impairment, or memory deterioration, and so forth.[5] Thus, early diagnosis and treatment are of great importance for patients with HSE to potentially decrease mortality.

In recent years, CT and MR imaging have been widely used in the early diagnosis of HSE. MR imaging has been reported to be superior to CT in revealing the characteristics of lesions, especially sequences such as T2 FLAIR and DWI.[6-8] Typically, HSE lesions are readily identified on such images (especially T2 FLAIR sequences). However, the conventional MR imaging appearance of HSE sometimes mimics other diseases, such as acute ischemic stroke,[9] mitochondrial encephalopathy with lactic acidosis and stroke-like episodes (MELAS),[10] or even diffuse low-grade glioma,[11] when the clinical presentations overlapping with other more common diseases are atypical.

Received June 25, 2019; accepted after revision August 26.

From the School of Medicine (R.L., L.M.), Nankai University, Tianjin, China; Department of Radiology (R.L., T.-F.L., Y.L., Y.W., K.W., X.-J.C., H.-F.X., Y.-L.W., L.M., X.L.), Chinese People's Liberation Army General Hospital, Beijing, China; and Department of Endocrinology (P.-A.S.), Cangzhou Central Hospital, Cangzhou, Hebei, China.

Please address correspondence to Lin Ma, MD, PhD, Department of Radiology, Chinese PLA General Hospital, 28 Fuxing Rd, Beijing 100853, China; e-mail: cjr.malin@vip.163.com

http://dx.doi.org/10.3174/ajnr.A6279

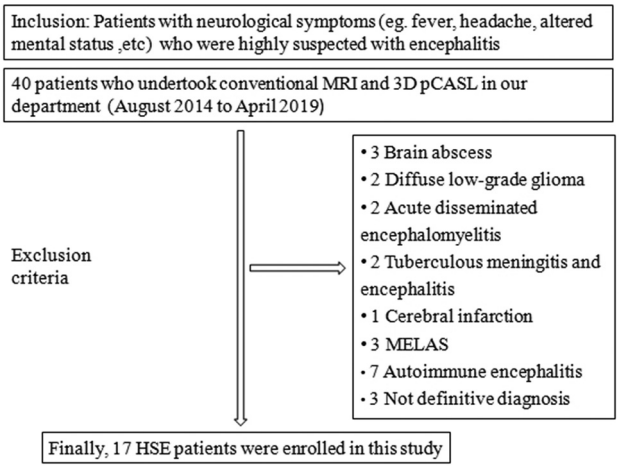

FIG 1. Flow chart showing the selection of the final study population. A total of 40 patients who underwent both conventional MR imaging and 3D-pCASL were clinically suspected of having encephalitis. Finally, 17 cases with HSE were included in this study.

Arterial spin-labeling (ASL) perfusion imaging is a completely noninvasive MR imaging technique for quantitative evaluation of CBF without exogenous injection of contrast agent.[12,13] The advantages and benefits of ASL have made it widely applied in evaluating brain perfusion in healthy populations (even in children and pregnant women), patients with renal insufficiency, and those who need repeat follow-up examinations.[13,14] Previous studies have shown that ASL has been widely applied in the diagnosis and differential diagnosis of many diseases, such as brain tumors,[15] stroke,[16] MELAS,[17] and so forth. Moreover, 3D pseudocontinuous ASL (pCASL) has combined the advantages of continuous ASL and pulsed ASL and has been recommended as standardized implementation for clinical applications.[12] However, few studies have yet been reported on the investigation of the perfusion appearance of HSE using 3D-pCASL.

Thus, the aim of this study was to retrospectively investigate the potential role of 3D-pCASL perfusion in HSE.

MATERIALS AND METHODS

Study Population

From August 2014 to April 2019, a total of 17 consecutive patients (12 males and 5 females; from 17 to 64 years of age; mean, 37.4 years) with a definite diagnosis of HSE were enrolled. A detailed flow chart of the study is shown in Fig 1. HSE was diagnosed according to the following criteria:[18,19] 1) acute or subacute onset of neurologic symptoms (eg, fever, disturbance of consciousness, seizure, and so forth); 2) abnormal findings on MR imaging; 3) CSF white blood cell count of $\geq 5/mm^3$; 4) virologic examination (including HSV DNA or increased HSV antibody level in CSF/serum or viral culture); 5) abnormal findings on an electroencephalogram; 6) empiric acyclovir and/or corticosteroid treatment being effective; and 7) exclusion of other encephalitis or other CNS diseases mimicking HSE.

The control group included 15 healthy volunteers (9 men and 6 women; age range, 20–60 years; mean, 36.8 years) imaged during the same period. The inclusion criteria were as follows: 1) roughly matched for age and sex with HSE subjects ($P > .05$); 2) no history of headache, epilepsy, head trauma, and other medical conditions affecting cerebral blood perfusion; and 3) normal findings on routine neurologic and conventional MR imaging examinations.

This study was approved by the PLA General Hospital ethics committee, and informed consent was also obtained. The healthy subject and patient information were anonymized during image analyses to protect privacy.

Inclusion/Exclusion Criteria for Study Patients

Patients were included in our study if they conformed to the above diagnostic criteria for HSE and had no history of other encephalitis, were admitted and treated at PLA General Hospital and underwent MR imaging, including conventional MR imaging and 3D-pCASL. On the contrary, patients were excluded from our study if HSE was suspected clinically without a final definite diagnosis; HSE was diagnosed on the basis of clinical criteria, but without abnormal findings on MR imaging; MR imaging had obvious motion artifacts or unusable images; and 3D-pCASL perfusion was not performed.

Conventional MR Imaging and 3D-pCASL

MR images were acquired on a 3T MR imaging system (Discovery 750; GE Healthcare, Milwaukee, Wisconsin) using a receive-only 32-channel phased-array head coil. Conventional MR imaging included T2WI (TR/TE = 4252/103.7 ms, FOV = 24 × 24 cm, matrix = 192 × 192, NEX = 1.5), T1WI (TR/TE/TI = 1750/24/780 ms, FOV = 24 × 24 cm, matrix = 320 × 320, NEX = 1), DWI (TR/TE = 6000/65.7 ms, FOV = 24 × 24 cm, matrix = 192 × 192, NEX = 2), and coronal and axial T2 FLAIR (TR/TE/TI = 8500/163/2100 ms, FOV = 24 × 24 cm, matrix = 288 × 224, NEX = 1). These images were obtained with identical section thickness (5 mm) and section space (1.5 mm). Postcontrast T1WI included axial, coronal, and sagittal planes (Magnevist, 0.1 mmol/kg, Bayer HealthCare Pharmaceuticals, Wayne, New Jersey).

3D-pCASL was acquired using a background-suppressed 3D spiral FSE technique. The parameters were as follows: TR/TE = 4844/10.5 ms, postlabeling delay = 2025 ms, FOV = 24 × 24 cm, section thickness = 4.0 mm, number of sections = 36, NEX = 3. In addition, a 3D T1-weighted fast-spoiled gradient recalled sequence was also obtained after contrast injection as an anatomic reference with TR/TE = 6.4/3.0 ms, FOV = 24 × 24 cm, section thickness = 4.0 mm, number of sections = 36, NEX = 1. Follow-up 3D-pCASL examinations were performed in patients 1, 2, 3, and 4 (Table 1).

Quantitative CBF Measurement and Normalized CBF

In this study, the lesions were classified into 3 categories according to the time from neurologic symptom onset to MR imaging evaluation. The acute stage of the lesion was up to 14 days from onset of symptoms; the subacute stage, from 15 to 25 days; and any duration beyond 26 days, the chronic stage.

ASL was postprocessed by functional software on a ADW4.5 workstation (GE Healthcare) to automatically generate CBF maps for every patient and all control individuals. For each patient, ROIs (28–40 mm^2) were manually and carefully placed within the lesions on CBF maps. The postcontrast 3D T1 fast-spoiled gradient recalled sequence, for accurate anatomic reference, was used

Table 1: Summary of the demographic and clinical features of consecutive patients with HSE

Case No.	Age (yr)	Sex	Clinical Presentation	Time (Days)[a]
1	17	M	Headache, fever, sudden unconscious attack, seizure	11/24/30
2	58	M	Headache, left lower extremity weakness and involuntary movement	4/14/20
3	35	M	Headache, nausea, vomiting, and memory deterioration	6/42
4	49	F	Headache and fever with irrelevant answer	2/17/29
5	21	F	Headache, fever, slow response, and memory deterioration	14
6	27	M	Persistent vertigo with sudden onset of left lower extremity weakness	26
7	32	M	Headache, fever, and seizure	7
8	28	M	Headache, dizziness, and memory deterioration	2
9	44	F	Memory deterioration, slow response	7
10	50	M	Headache, fever, dizziness, paroxysmal loss of consciousness, seizure	3
11	20	F	Fever, disturbance of consciousness with limb seizure	5
12	47	F	Headache, fever, behavioral and psychological disorder	15
13	47	M	Headache, fever, dizziness	20
14	26	M	Headache and fever with paroxysmal limb seizure	15
15	25	M	Recurrent fever, paraphasia, memory deterioration, and limb seizure	85
16	46	M	Headache, fever, convulsion with psychological and behavioral disorder	60
17	64	M	Headache, dizziness, memory deterioration, paroxysmal loss of consciousness, and seizure	6

[a] The time from symptom onset to 3D-pCASL evaluation.

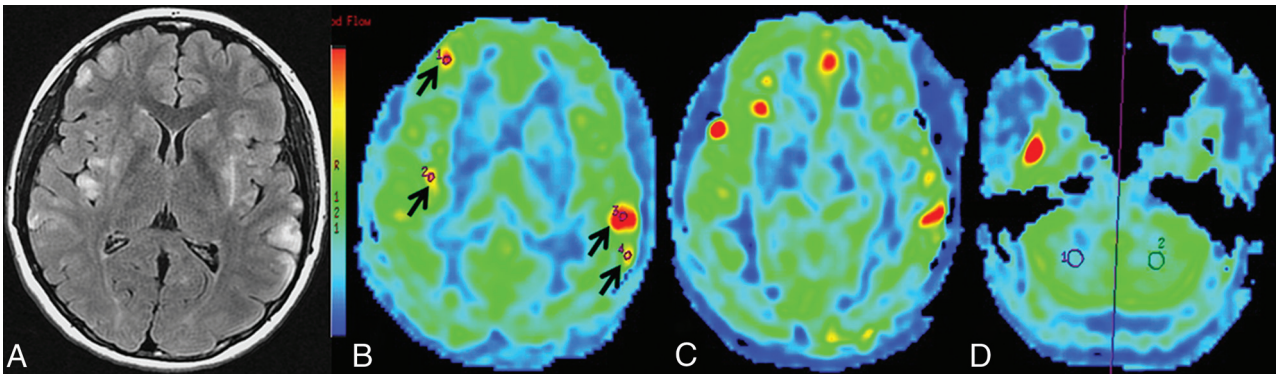

FIG 2. Case 11, a 20-year-old female patient at the acute stage (5 days after the onset of symptoms). *A*, Axial T2 FLAIR shows multiple lesions located in right frontal and bilateral insular lobes, as well as the bilateral temporal lobes. *B*, 3D-pCASL demonstrates increased CBF, consistent with involved regions on axial T2 FLAIR (*black arrows*). *C*, Other lesions also show hyperperfusion in different affected areas. *D*, ROI site selection for bilateral cerebellum CBF on the pCASL CBF color map.

for image registration with 3D-pCASL. Then 3D T1 fast-spoiled gradient recalled and T2 FLAIR images were cross-referenced for the lesion location. For each healthy individual, 3–5 round ROIs were placed in the temporal cortex as control group. To minimize individual differences, we applied the normalized CBF in this study. Previous studies have shown that cerebellar perfusion is relatively stable;[15,20] in addition, HSE rarely involves the cerebellum. Thus, the intraindividual normalization with the cerebellum was used. The nCBF value was defined as the CBF value of the lesions or the normal cortex in the temporal lobe divided by the mean CBF value in the cerebellum (nCBF = CBF lesion or temporal cortex/mean CBF cerebellum). The ROIs (approximately 100 mm^2) were positioned in the bilateral cerebellar hemispheres (Fig 2*D*), and the mean value was regarded as the final reference.

The ROIs were drawn by 2 neuroradiologists with >10 years' experience who were unaware of the clinical information and blinded to scan time points of the patients.

Statistical Analysis

Statistical analyses were performed with SPSS for Windows (Version 20.0; IBM, Armonk, New York). For each patient, the mean CBF value was acquired and calculated from all lesion foci. We compared the mean nCBF values of different stages with those of the control group. If 2 independent continuous variables complied with a normal distribution, the Student *t* test was used; otherwise, the Mann–Whitney *U* test was performed. Comparison among acute, subacute, and chronic stages was not performed. Interobserver variability assessments were evaluated with the intraclass correlation coefficient. The intraclass correlation coefficient was interpreted as follows: poor (<0.4), fair (0.4–0.59), good (0.6–0.74), and excellent (>0.74). $P < .05$ was considered statistically significant.

RESULTS

Patient Population

Demographic and clinical features of 17 consecutive patients with HSE are summarized in Table 1. On the basis of the laboratory tests, the causative agent was HSV-1 in all cases. Clinical manifestations were mainly such symptoms as headache ($n = 13$, 76.5%), fever ($n = 11$, 64.7%), seizure ($n = 8$, 47.1%), memory deterioration ($n = 6$, 35.3%), altered level of consciousness ($n = 4$, 23.5%),

Table 2: Initial conventional MR imaging and ASL findings after admission in patients with HSE

Case No.	Lesion Location[a]	T2WI	T1WI	CE	Perfusion[b]
1	L. T	Slight hyper/hypo	Slight hypo/hyper	NA	Obvious hyper
2	L. T, I	Slight hyper	Slight hypo/hyper	Gyriform enhancement	Obvious hyper
3	L. T, I	Slight hyper	Slight hypo/hyper	Patchy enhancement	Obvious hyper
4	R. F, T	Slight hyper	Slight hypo	None	Obvious hyper
5	L. F, I, and Bil. T	Slight hyper/hyper	Slight hypo/hyper	Gyriform enhancement	Obvious hyper
6	Bil. T, and R. P	Slight hyper/hyper	Slight hypo/hyper	None	Slight hypo
7	L. F, P, O, and Bil. I, T	Slight hyper	Iso	Patchy enhancement	Slight hyper/hyper
8	Bil. T, and L. I	Slight hyper	Slight hypo	None	Obvious hyper
9	Bil. F, T, I	Slight hyper	Slight hypo	None	Obvious hyper
10	Bil. F and cingulate gyrus	Slight hyper	Iso	None	Obvious hyper
11	R. F, and Bil. T, I	Slight hyper	Iso	None	Obvious hyper (multiple lesions)
12	Bil. F, T, I, and cingulate gyrus	Slight hyper	Slight hypo	Patchy enhancement	Obvious hyper
13	R. T, and Bil. I	Slight hyper	Slight hypo	Slight meningeal enhancement	Regional hyper
14	L. T, I	Slight hypo/hyper	Slight hypo/hyper	Gyriform enhancement	Regional hyper
15	L. T, I	Slight hyper/hyper	Slight hypo/hypo	Slight gyriform enhancement	Obvious hypo
16	R. T, I	Slight hyper/hyper	Slight hypo/hypo	Slight enhancement	Obvious hypo
17	R. T, I	Slight hyper	Slight hypo	None	Obvious hyper

Note:— R indicates right; L, left; Bil., bilateral; F, frontal lobe; T, temporal lobe; P, parietal lobe; O, occipital lobe; I, insular lobe; hyper, hyperintensity or hyperperfusion; hypo, hypointensity or hyperperfusion; Iso, isointensity; CE, contrast enhancement; NA, not applicable.

[a] Abnormal signals on T2 FLAIR.

[b] Perfusion performance on the first ASL examination.

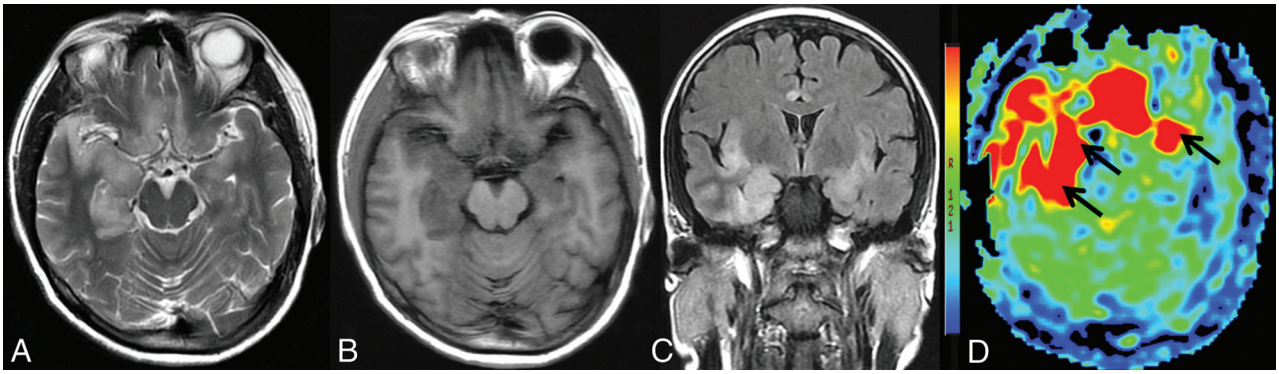

FIG 3. Case 12, a 47-year-old female patient at the subacute stage (15 days after the onset of symptoms). *A*, Axial T2WI shows hyperintensities in bilateral frontal, temporal, and insular lobes and the cingulate gyrus. *B*, Axial T1WI demonstrates slight hypointensities. *C*, Slight hyperintensities are observed on coronal T2 FLAIR. *D*, 3D-pCASL shows high perfusion (*black arrows*) in the corresponding involved areas.

vertigo/dizziness ($n = 4$, 23.5%), behavioral and psychological disorder ($n = 2$, 11.8%), and nausea/vomiting ($n = 1$, 5.9%). The time from the onset of symptoms to the first 3D-pCASL scan ranged from 2 to 85 days (median time, 7 days) (Table 1).

Conventional MR Imaging Features

Table 2 summarizes the location of lesions and conventional MR imaging findings. The lesions were asymmetrically distributed bilaterally (52.9%) in 9 patients (patients 5, 6, 7, 8, 9, 10, 11, 12, and 13) and unilaterally (47.1%) in 8 patients (patients 1, 2, 3, 4, 14, 15, 16, and 17). The involved locations mainly included the temporal, frontal, and insular lobes; hippocampal region; and cingulate gyrus. The basal ganglia and cerebellum were spared in all cases.

ASL–MR Imaging Evaluation

By empiric visual inspection, 14 of 17 patients with HSE showed increased CBF in the affected regions on the initial 3D-pCASL scan, except for patients 6, 15, and 16 with hypoperfusion (Table 2). On the basis of the duration between the onset of symptoms and brain MR imaging, 11 cases were judged to be at the acute stage; 6 cases, at the subacute stage; and 6 cases, at the chronic stage. HSE demonstrated hyperperfusion in the acute (Fig 2) and subacute (Fig 3) stages, whereas it showed hypoperfusion in the chronic stage on 3D-pCASL (Fig 4*L*).

Interobserver reproducibility of CBF values was performed, and intraclass correlation coefficients were 0.92 at the acute stage, 0.90 at the subacute stage, 0.79 at the chronic stage, and 0.81 in the control group, respectively.

The mean CBF values of lesions in HSE were 121.5 ± 33.8 mL/100g/min (range, 59.5–162.3 mL/100g/min) in the acute stage, 98.3 ± 22.8 mL/100g/min (range, 66.1–126.5 mL/100g/min) in the subacute stage, and 33.9 ± 15.0 mL/100g/min (range, 23.0–63.1 mL/100g/min) in the chronic stage, respectively (Table 3). The mean nCBF values of lesions for different stages were 2.68 ± 0.54, 2.42 ± 0.52, and 0.87 ± 0.30 mL/100g/min at acute, subacute, and chronic stages, respectively (Table 3).

The mean nCBF values of acute and subacute lesions were significantly higher than those for the control group (both, $P < .001$), whereas the mean nCBF values of chronic lesions were lower than those of the control group ($P < .05$) (Fig 5*A*).

Serial 3D-pCASL was performed in 4 patients (patients 1–4), showing the time course of mean CBF changes of the lesions at different time points (Fig 5*B*) and dynamic perfusion reduction with time after treatment (Fig 4).

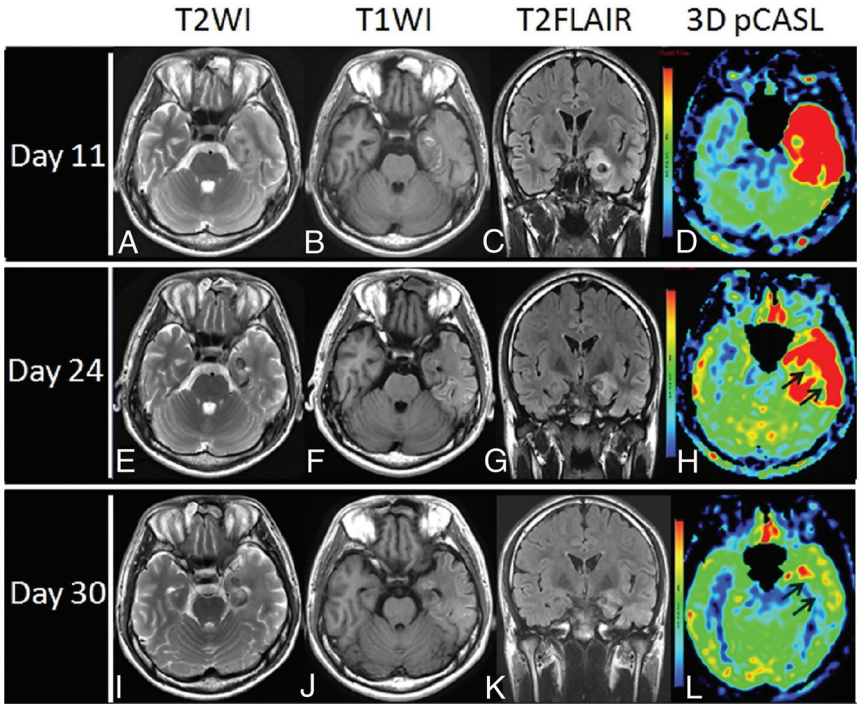

FIG 4. Case 1, a 17-year-old male patient. Serial T2WI (*A*, *E*, and *I*), T1WI (*B*, *F*, and *J*), and coronal T2 FLAIR (*C*, *G*, and *K*) demonstrate abnormal signals on the left temporal lobe and hippocampus. Serial follow-up 3D-pCASL perfusion imaging was performed, which reveals dynamic changes in the involved area on the 11th (*D*), 24th (*H*), and 30th day (*L*), respectively (*black arrows*). Meanwhile, the patient's condition markedly improved with effective therapeutic intervention.

Table 3: Mean CBF and mean nCBF values in the lesions at different stages and control group findings

Stage (Days)	No. of Cases	Range of CBF Values (mL/100g/min)	Mean CBF Values (mL/100g/min)	Mean nCBF Values
Acute stage (≤14)	11	59.5–162.3	121.5 ± 33.8	2.68 ± 0.54
Subacute stage (15–25)	6	66.1–126.5	98.3 ± 22.8	2.42 ± 0.52
Chronic stage (≥26)	6	23.0–63.1	33.9 ± 15.0	0.87 ± 0.30
Control group[a]	15	47.9–71.9	58.8 ± 7.0	1.33 ± 0.08

[a] The temporal cortex perfusion as a control reference.

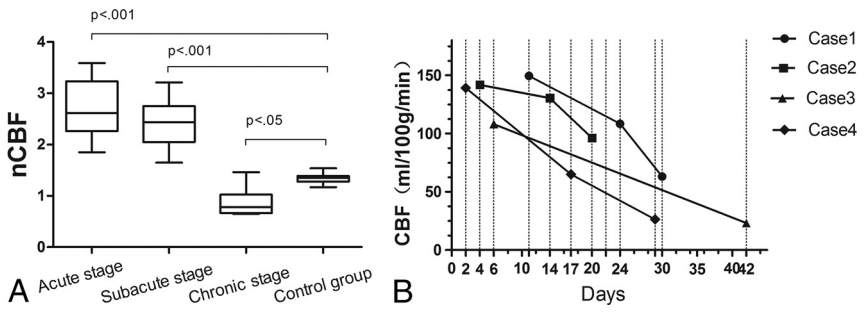

FIG 5. *A*, The boxplot of nCBF values in acute-, subacute-, and chronic-stage lesions and the control group, respectively. *B*, Time course of mean CBF changes for lesions at different time points in 4 follow-up HSE cases. The mean CBF value of the lesions gradually decreased after treatment in 4 case series.

DISCUSSION

In the present study, we explored the potential characteristics of 3D-pCASL perfusion in HSE. Our principal findings can be summarized as follows: 1) By visual assessment, patients with HSE demonstrated increased CBF in the affected area in the acute and subacute lesions, while CBF decreased in chronic lesions on 3D-pCASL; 2) quantitative analysis indicated that the nCBF values of acute and subacute lesions were obviously higher, whereas the nCBF values of chronic lesions were lower compared with the control group; and 3) follow-up 3D-pCASL examinations in 4 patients showed dynamic perfusion alterations with decreased perfusion after therapy.

HSE is a serious brain infection with high rates of mortality and morbidity, without timely and effective treatment.[21,22] The most important evidence in the diagnosis of HSE includes neurologic signs and symptoms and electroencephalogram and laboratory examinations. In clinical practice, once HSE is strongly suspected, the work-up must be initiated immediately and empiric antiviral therapy should be adopted promptly. However, the diagnosis is often delayed, and the main reason for the delay in the initiation of treatment is that the differential diagnosis should be made while waiting for the results of CSF polymerase chain reaction analysis.[23] Although virologic tests and pathologic biopsy are considered the criterion standard for the diagnosis of HSE, the former is relatively slow and has high false-negative rates within the initial few days[21] and the latter needs an invasive neurosurgical procedure, which is not widely accepted and applied in clinical practice.

Neuroimaging examinations may demonstrate characteristic findings of HSE and are of great importance in the differential diagnosis. As reported

in the literature,[5,11,24] our results also demonstrated that the lesions on conventional MR imaging manifest as an asymmetric involvement of the temporal lobes. Other brain regions, such as frontal lobes, insular lobes, hippocampus region, and cingulate cortex, might also be affected, while the basal ganglia region and cerebellum are rarely involved.[24] Routine MR images including T1WI, T2WI, T2 FLAIR, DWI, and postcontrast images are most important in identifying brain abnormalities in HSE.

Perfusion imaging has been widely applied in research and clinical practice to provide more information in various neurologic disorders.[25] Previous perfusion studies, either CTP[26] or SPECT,[27,28] have been reported for HSE, showing focal CBF abnormalities in the affected regions, but they are less often used in routine clinical practice because of contrast agent administration and radiation exposure. So far, 3D-pCASL perfusion alterations in HSE have not been well-described. Noguchi et al[29] have reported the application of ASL-MR imaging in central nervous system infections (including only 3 patients with HSE), with the results indicating that HSE showed high perfusion on ASL only by visual assessment without quantitative analysis. In this study, we found that the hyperintense lesions on T2 FLAIR demonstrated hyperperfusion in acute and subacute stages and hypoperfusion in the chronic stage.

The exact mechanism of increased CBF in the affected region of HSE has not been elucidated. We speculated that in the acute and subacute stages, angiitis due to direct invasion of HSV might cause blood vessel dilation,[30] resulting in increased metabolism and increased regional CBF. In the chronic stage, however, focal hypoperfusion in the involved areas was found possibly due to neuronal excessive damage and loss of brain parenchyma caused by a series of direct virus-mediated and indirect immune-mediated responses.[31] In addition, we also observed the quantitative perfusion alterations after appropriate therapy in 4 longitudinal HSE cases (Fig 5*B*). We found that high-perfusion lesions at the acute stage gradually evolved to low-perfusion areas with time, indicating that treatment may be effective (Fig 4).

Previous research has shown that perfusion alterations in patients with acute and subacute encephalitis have been correlated with clinical status, including seizure and clinical outcome.[30] Normal CBF in the subacute phase usually indicates a good neurologic outcome 1 year after the acute illness.[32] Moreover, we think 3D-pCASL perfusion can be helpful in the differential diagnosis among HSE, infarct, MELAS, and low- and high-grade gliomas, especially at the acute stage. Most important, acute infarct demonstrates hypoperfusion, which can be reliably differentiated from early HSE. MELAS initially misdiagnosed as HSE has been reported,[10] and both show hyperperfusion, while hyperperfusion is mainly located in the cortical region in MELAS.[17] MELAS and high-grade glioma, mimicking early HSE, present with hyperperfusion on 3D-pCASL, but differentiation can be made by combining the clinical manifestation, history, lesion location, and so forth.

According to the current guidelines,[21] it is generally recommended that the antiviral treatment be implemented in highly suspected HSE without the results of the CSF test. Our study found that hyperperfusion was observed in the affected area in the acute and subacute lesions in patients with HSE. If radiologists suggest the HSE diagnosis based on the ASL perfusion feature in the appropriate clinical setting, clinicians could be afforded the chance to start an immediate intervention before the results of laboratory tests are confirmed, which may give the patient a better prognosis. Therefore, we would expect that the initial 3D-pCASL after admission be performed as early as possible to diagnose and differentiate HSE from other neurologic disorders.

Besides its retrospective nature, some limitations of our study merit consideration. First, the sample size was relatively small, and serial 3D-pCASL was performed in only 4 patients, though the trends in perfusion changes were shown, with potential implications for follow-up evaluation and therapy monitoring. Second, other types of encephalitis and infectious diseases were not included in this study. Further investigation is required to establish the perfusion differences among different types of encephalitis.

CONCLUSIONS

Conventional MR imaging remains the optimal technique in the early diagnosis of HSE; however, we believe that 3D-pCASL can be used as an important adjunctive technique and that high perfusion in the lesion does add valuable information in diagnosing HSE, especially at the acute stage. Serial 3D-pCASL has a potential value in the evaluation of the therapeutic effect of HSE.

REFERENCES

1. Kiroğlu Y, Calli C, Yunten N, et al. **Diffusion-weighted MR imaging of viral encephalitis.** *Neuroradiology* 2006;48:875–80 CrossRef Medline
2. Choradia M, Rastogi H. **Viral encephalitis: imaging features.** *Apollo Medicine* 2008;5:111–17 CrossRef
3. Granerod J, Ambrose HE, Davies NW, et al. **Causes of encephalitis and differences in their clinical presentations in England: a multicentre, population-based prospective study.** *Lancet Infect Dis* 2010; 10:835–44 CrossRef Medline
4. Solomon T, Hart IJ, Beeching NJ. **Viral encephalitis: a clinician's guide.** *Pract Neurol* 2007;7:288–305 CrossRef Medline
5. Sili U, Kaya A, Mert A; HSV Encephalitis Study Group. **Herpes simplex virus encephalitis: clinical manifestations, diagnosis and outcome in 106 adult patients.** *Clin Virol* 2014;60:112–18 CrossRef Medline
6. Noguchi T, Yoshiura T, Hiwatashi A, et al. **CT and MRI findings of human herpesvirus 6-associated encephalopathy: comparison with findings of herpes simplex virus encephalitis.** *AJR Am J Roentgenol* 2010;194:754–60 CrossRef Medline
7. Sawlani V. **Diffusion-weighted imaging and apparent diffusion coefficient evaluation of herpes simplex encephalitis and Japanese encephalitis.** *J Neurol Sci* 2009;287:221–26 CrossRef Medline
8. Misra UK, Kalita J, Phadke RV, et al. **Usefulness of various MRI sequences in the diagnosis of viral encephalitis.** *Acta Tropica* 2010;116:206–11 CrossRef Medline
9. Hara Y, Ishii N, Sakai K, et al. **Herpes simplex encephalitis initially presented with parietal cortex lesions mimicking acute ischemic stroke: a case report [in Japanese].** *Rinsho Shinkeigaku* 2016;56:104–07 CrossRef Medline
10. Gooriah R, Dafalla BE, Venugopalan TC. **Led astray: MELAS initially misdiagnosed as herpes simplex encephalitis.** *Acta Neurol Belg* 2015;115:789–92 CrossRef Medline

11. Eran A, Hodes A, Izbudak I. **Bilateral temporal lobe disease: looking beyond herpes encephalitis.** *Insights Imaging* 2016;7:265–74 CrossRef Medline
12. Alsop DC, Detre JA, Golay X, et al. **Recommended implementation of arterial spin-labeled perfusion MRI for clinical applications: a consensus of the ISMRM perfusion study group and the European consortium for ASL in dementia.** *Magn Reson Med* 2015;73:102–16 CrossRef Medline
13. Petcharunpaisan S, Ramalho J, Castillo M. **Arterial spin labeling in neuroimaging.** *World J Radiol* 2010;2:384–98 CrossRef Medline
14. Detre JA, Rao H, Wang DJ, et al. **Applications of arterial spin labeled MRI in the brain.** *J Magn Reson Imaging* 2012;35:1026–37 CrossRef Medline
15. Xiao HF, Chen ZY, Lou X, et al. **Astrocytic tumour grading: a comparative study of three-dimensional pseudocontinuous arterial spin labelling, dynamic susceptibility contrast-enhanced perfusion-weighted imaging, and diffusion-weighted imaging.** *Eur Radiol* 2015;25:3423–30 CrossRef Medline
16. Bokkers RP, Hernandez DA, Merino JG, et al. **Whole-brain arterial spin labeling perfusion MRI in patients with acute stroke.** *Stroke* 2012;43:1290–94 CrossRef Medline
17. Li R, Xiao HF, Lyu JH, et al. **Differential diagnosis of mitochondrial encephalopathy with lactic acidosis and stroke-like episodes (MELAS) and ischemic stroke using 3D pseudocontinuous arterial spin labeling.** *J Magn Reson Imaging* 2017;45:199–206 CrossRef Medline
18. Venkatesan A, Tunkel AR, Bloch KC, et al; International Encephalitis Consortium. **Case definitions, diagnostic algorithms, and priorities in encephalitis: consensus statement of the international encephalitis consortium.** *Clin Infect Dis* 2013;57:1114–28 CrossRef Medline
19. Singh TD, Fugate JE, Hocker S, et al. **Predictors of outcome in HSV encephalitis.** *J Neurol* 2016;263:277–89 CrossRef Medline
20. Arbab AS, Aoki S, Toyama K, et al. **Brain perfusion measured by flow-sensitive alternating inversion recovery (FAIR) and dynamic susceptibility contrast-enhanced magnetic resonance imaging: comparison with nuclear medicine technique.** *Eur Radiol* 2001; 11:635–41 CrossRef Medline
21. Kennedy PG, Steiner P. **Recent issues in herpes simplex encephalitis.** *J Neurovirol* 2013;19:346–50 CrossRef Medline
22. Jha S, Patel R, Yadav RK, et al. **Clinical spectrum, pitfalls in diagnosis and therapeutic implications in herpes simplex encephalitis.** *J Assoc Physicians India* 2004;52:24–26 Medline
23. Hughes PS, Jackson AC. **Delays in initiation of acyclovir therapy in herpes simplex encephalitis.** *Can J Neurol Sci* 2012;39:644–48 CrossRef Medline
24. Adam G, Ferrier M, Patsoura S, et al. **Magnetic resonance imaging of arterial stroke mimics: a pictorial review.** *Insights Imaging* 2018; 9:815–31 CrossRef Medline
25. Essig M, Nguyen TB, Shiroishi MS, et al. **Perfusion MRI: the five most frequently asked clinical questions.** *AJR Am J Roentgenol* 2013;201:W495–510 CrossRef Medline
26. Marco de Lucas E, G, Mandly A, Gutierrez A, et al. **Computed tomography perfusion usefulness in early imaging diagnosis of herpes simplex virus encephalitis.** *Acta Radiol* 2006;47:878–81 CrossRef Medline
27. Launes J, Nikkinen P, Lindroth L, et al. **Diagnosis of acute herpes simplex encephalitis by brain perfusion single photon emission computed tomography.** *Lancet* 1988;1:1188–91 Medline
28. De Deyn PP, Van den Broucke PW, Pickut BA, et al. **Perfusion and thallium single photon emission computed tomography in herpes simplex encephalitis.** *J Neurol Sci* 1998;157:96–99 CrossRef Medline
29. Noguchi T, Yakushiji Y, Nishihara M, et al. **Arterial spin-labeling in central nervous system infection.** *Magn Reson Med Sci* 2016;15:386–94 CrossRef Medline
30. Wong AM, Yeh CH, Lin JJ, et al. **Arterial spin-labeling perfusion imaging of childhood encephalitis: correlation with seizure and clinical outcome.** *Neuroradiology* 2018;60:961–70 CrossRef Medline
31. Chucair-Elliott AJ, Conrady C, Zheng M, et al. **Microglia-induced IL-6 protects against neuronal loss following HSV-1 infection of neural progenitor cells.** *Glia* 2014;62:1418–34 CrossRef Medline
32. Kao CH, Wang SJ, Mak SC, et al. **Viral encephalitis in children: detection with technetium-99m HMPAO brain single-photon emission CT and its value in prediction of outcome.** *AJNR Am J Neuroradiol* 1994;15:1369–73 Medline